Nuclear magnetic resonance study of diffusion and localised motion of H(D) atoms in $TaV_2H_x(D_x)$

1990 J. Phys.: Condens. Matter 2 7195

(http://iopscience.iop.org/0953-8984/2/34/013)

J. Phys.: Condens. Matter 2 (1990) 7195–7208. Printed in the UK

Nuclear magnetic resonance study of diffusion and localised motion of H(D) atoms in $TaV_2H_x(D_x)$

A V Skripov, S V Rychkova, M Yu Belyaev and A P Stepanov
Institute of Metal Physics, Urals Branch of the Academy of Sciences, Sverdlovsk 620219, USSR

Received 19 February 1990

Abstract. Nuclear magnetic resonance measurements of ^1H, ^2D and ^{51}V spin-lattice relaxation rates T_1^{-1} in $TaV_2H_x(D_x)$ ($0.22 \leq x \leq 1.54$) have been performed over the temperature range 10–440 K. For all the studied samples the double-peak temperature dependence of T_1^{-1} is observed. The high-temperature relaxation rate maximum is associated with H(D) diffusion, and the low-temperature one is attributed to localised motion of H(D) atoms. The experimental results are analysed to obtain the parameters of the two types of motion as functions of temperature and H(D) content. At 300 K the diffusion rate is found to increase with increasing H(D) concentration. The characteristic period of the localised motion, τ_L, exhibits unusual temperature dependence, $\tau_L \sim \exp(-T/T_0)$ with $T_0 \simeq 50$ K.

1. Introduction

The problem of hydrogen diffusion in Laves phase hydrides has received much recent attention [1–5]. In this class of materials the temperature dependences of the measured ^1H spin relaxation times T_1 and $T_{1\rho}$ show strong deviations from the predictions based on the Arrhenius-type behaviour of hydrogen mobility. In some cases the nuclear spin relaxation data could be accounted for in terms of the model [1, 5] implying a coexistence of two types of hydrogen motion with different frequency scales. However, until recently direct evidence for such a coexistence in Laves phase hydrides was lacking. In previous NMR studies [6, 7] we have found the unusual localised motion of H(D) atoms in the C15-type compound TaV_2. The localised motion coexists with much slower long-range diffusion and gives rise to the additional low-temperature maximum of the spin-lattice relaxation rate T_1^{-1}. A similar low-temperature T_1^{-1} maximum has recently been found in α-ScH_x [8] and α-LuH_x [9].

TaV_2 is known to absorb considerable amounts of hydrogen (up to 1.8 H atoms per formula unit) [10]. At room temperature hydrogen absorption does not affect the host structure, giving rise only to lattice expansion. However, the complete phase diagram of the TaV_2–H(D) system is not known. According to the neutron diffraction data [11] hydrogen atoms in TaV_2 occupy tetrahedral interstitial sites of the g-type, formed by 2V and 2Ta atoms. In the present work we report on the studies of ^1H, ^2D and ^{51}V spin-lattice relaxation rates in $TaV_2H_x(D_x)$ over wide ranges of temperature and hydrogen concentration. The aim of these studies is to clarify the nature of H(D) motion in TaV_2 and the behaviour of motional parameters as functions of temperature and H(D) content. Some preliminary results have been published in our previous letter [7].

0953-8984/90/347195 + 14 $03.50

2. Experimental details

The preparation of the samples has been described elsewhere [7]. Measurements were made on powdered samples of TaV_2H_x ($x = 0.22$, 0.56, 0.70, 0.87, 1.15 and 1.33) and TaV_2D_x ($x = 0.50$, 0.84, 1.08 and 1.54). X-ray diffraction studies have shown that at room temperature all the samples are single-phase solid solutions with the cubic C15-type host-metal structure. The lattice parameter a_0 changes from 7.172 Å ($x = 0.22$) to 7.326 Å ($x = 1.54$). The single-phase state with the C15 host structure is retained down to 80 K.

NMR measurements were performed on a Bruker SXP pulse spectrometer at the frequencies $\omega/2\pi = 13.8$ MHz (^{2}D), 19.3 MHz (^{51}V and ^{1}H), and 31, 64 and 90 MHz (^{1}H). Spin-lattice relaxation times T_1 were determined from the recovery of free induction decay (FID) signal after the saturation pulse sequence (^{51}V) or after a single RF pulse (^{1}H and ^{2}D). In all cases the recovery could be fitted by an exponential function.

The low-temperature measurements were made in an Oxford Instruments CF200 continuous flow helium cryostat. The sample temperature monitored by a chromel–(Au–Fe) thermocouple was stable to within 0.1 K. For $T > 290$ K we used a glass Dewar system with an air flow. In this range the temperature monitored by a Cu–constantan thermocouple was stable to within 0.5 K.

3. Results

As examples of the observed temperature dependences of ^{1}H spin-lattice relaxation rates we show in figure 1 the results of $(T_1^{-1})_H$ measurements in $TaV_2H_{0.87}$ and $TaV_2H_{1.15}$ at $\omega/2\pi = 90$ MHz. Similar double-peak $T_1^{-1}(T)$ dependences are observed for all the studied TaV_2H_x samples. The behaviour of ^{1}H NMR linewidths indicates that the high-

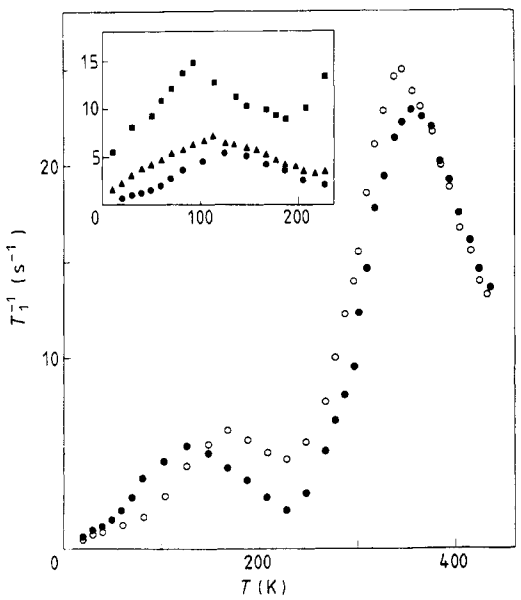

Figure 1. The temperature dependence of the ^{1}H spin-lattice relaxation rate in $TaV_2H_{0.87}$ (●) and $TaV_2H_{1.15}$ (○) measured at 90 MHz. Inset: the low-temperature part of the temperature dependence of $(T_1^{-1})_H$ in $TaV_2H_{0.87}$ at 31 (■), 64 (▲) and 90 MHz (●).

temperature $(T_1^{-1})_H$ maximum is due to diffusive motion of H atoms. Above 230 K the nuclear dipole–dipole interaction is dynamically averaged to zero, and ^{1}H NMR linewidth is determined only by the distribution of demagnetising fields. The low-temperature $(T_1^{-1})_H$ maximum can be attributed to localised motion of H atoms [6, 7]. This is supported by the low-temperature behaviour of $(T_1^{-1})_H$ at different frequencies (inset in figure 1), typical for motionally induced relaxation. As discussed in [7], we can exclude the possibilities that the low-T relaxation rate maximum originates from impurity effects or from hydrogen diffusion in the residual BCC phase. In metal–hydrogen systems the measured $(T_1^{-1})_H$ at low temperatures is usually dominated by the conduction-electron contribution T_{1e}^{-1}, which is frequency-independent and proportional to temperature. As can be seen from the inset in figure 1, in our case the strong frequency dependence is retained even at $T < 20$ K. This suggests that the localised motion of H atoms is not frozen on the NMR frequency scale down to very low temperatures.

In figure 2 we have plotted the $(T_1^{-1})_H$ values at the low-T maximum and at $T = 30$ K as functions of resonance frequency for $TaV_2H_{0.87}$. It can be seen that the corresponding frequency dependences are well described by $(T_1^{-1})_H^{LTmax} \sim \omega^{-1}$ and T_1^{-1} (30 K) $\sim \omega^{-2}$, as expected for the Bloembergen–Purcell–Pound (BPP) model [12] of motionally induced relaxation. This also implies that the conduction-electron contribution T_{1e}^{-1} is small in the region of the low-T peak.

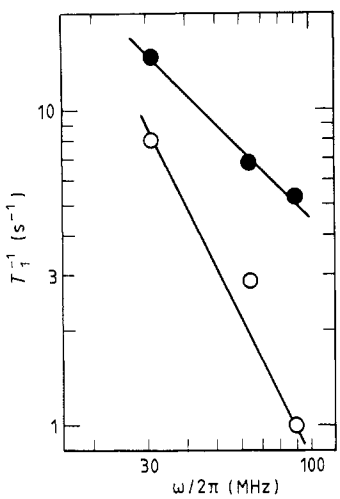

Figure 2. The proton spin-lattice relaxation rates at the low-T maximum (●) and at $T = 30$ K (○) in $TaV_2H_{0.87}$ as functions of resonance frequency. The full lines show the ω^{-1} and ω^{-2} dependences.

Figure 3 shows the temperature dependences of ^{51}V spin-lattice relaxation rates for $TaV_2D_{0.50}$ and $TaV_2D_{1.08}$. Similar double-peak temperature dependences of $(T_1^{-1})_V$ are observed for all the studied $TaV_2H_x(D_x)$ samples. As in the other vanadium-based Laves phase hydrides [3, 4], the $(T_1^{-1})_V$ peaks result from the electric quadrupole interaction modulated by H(D) motion. Since only charge fluctuations are important for this mechanism, H and D atoms are expected to give the same contributions to $(T_1^{-1})_V$ if their motional parameters are the same. The measured vanadium relaxation rates in $TaV_2H_{0.87}$ and $TaV_2D_{0.84}$ are compared in figure 4. It can be seen that the high-T maximum relaxation rates $(T_1^{-1})_V^{HTmax}$ for the two compounds are nearly the same, as

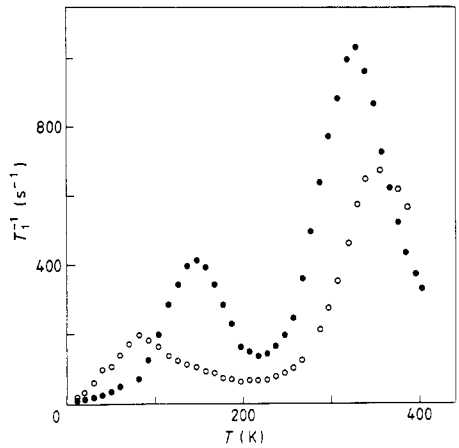

Figure 3. The temperature dependence of the ^{51}V spin-lattice relaxation rate in $TaV_2D_{0.50}$ (○) and $TaV_2D_{1.08}$ (●) measured at 19.3 MHz.

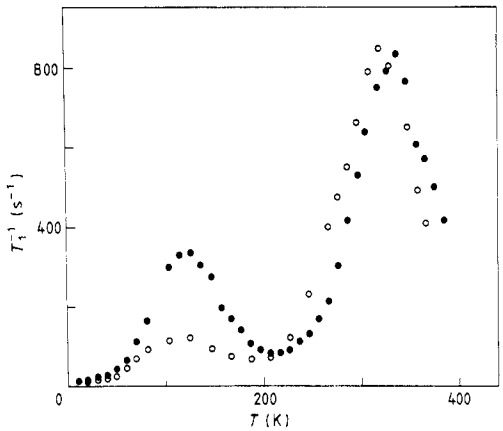

Figure 4. The temperature dependence of the ^{51}V spin-lattice relaxation rate in $TaV_2D_{0.84}$ (●) and $TaV_2H_{0.87}$ (○) measured at 19.3 MHz.

expected. The observed shift of the positions of the high-T maxima indicates the normal isotope effect in H(D) diffusion rate. The most striking feature of the ^{51}V relaxation data is the strong difference between the low-T maximum relaxation rates $(T_1^{-1})_V^{LTmax}$ for the hydrides and the deuterides with nearly the same x. As can be seen from figure 4, the $(T_1^{-1})_V^{LTmax}$ value for $TaV_2D_{0.84}$ is almost three times higher than for $TaV_2H_{0.87}$. A similar difference between the $(T_1^{-1})_V^{LTmax}$ values for the hydrides and the deuterides with nearly the same x is observed for all the studied H(D) concentrations. This means that the amplitude of electric field gradient (EFG) fluctuations at V sites in the deuterides is considerably higher than in the hydrides.

The conduction-electron contribution $(T_{1e}^{-1})_V$, which is normally proportional to temperature, can be estimated from the low-temperature parts of $(T_1^{-1})_V$ versus T plots and/or from the $(T_1^{-1})_V$ minima between the two peaks. The resulting values of $(T_{1e}T)_V^{-1}$ for different samples are presented in table 1. This table also lists the temperatures of the low-T and high-T maxima for ^{51}V relaxation rate and the maximum

Table 1. The ^{51}V relaxation parameters of $TaV_2H_x(D_x)$ measured at 19.3 MHz: the electronic contribution $(T_{1e}T)_V^{-1}$, the temperatures of low-T and high-T relaxation rate maxima, T_{LTmax} and T_{HTmax}, and the maximum motional relaxation rates, $(T_{1m}^{-1})_V^{LTmax}$ and $(T_{1m}^{-1})_V^{HTmax}$.

Sample	$(T_{1e}T)_V^{-1}$ (s^{-1} K^{-1})	T_{LTmax} (K)	$(T_{1m}^{-1})_V^{LTmax}$ (s^{-1})	T_{HTmax} (K)	$(T_{1m}^{-1})_V^{HTmax}$ (s^{-1})
$TaV_2H_{0.22}$	0.90	~50	~20	360	286
$TaV_2H_{0.87}$	0.38	103	77	320	728
$TaV_2H_{1.15}$	0.38	125	116	319	929
$TaV_2H_{1.33}$	0.39	147	125	310	1030
$Tav_2D_{0.50}$	0.30	81	184	356	571
$TaV_2D_{0.84}$	0.39	125	294	337	701
$TaV_2D_{1.08}$	0.45	147	351	328	885
$TaV_2D_{1.54}$	0.36	177	470		

motional contributions $(T_{1m}^{-1})_V^{LTmax}$ and $(T_{1m}^{-1})_V^{HTmax}$. The values of $(T_{1m}^{-1})_V$ are obtained by subtracting $(T_{1e}^{-1})_V$ from the measured $(T_1^{-1})_V$.

Since the measured ^1H relaxation rates exhibit strong frequency dependences even at very low temperatures, and for some x the two relaxation peaks are not well separated, it is difficult to estimate the electronic contributions $(T_{1e}^{-1})_H$. In order to obtain reasonable estimates of $(T_{1e}^{-1})_H$ we assume that, for all x, $(T_{1e}^{-1})_V/(T_{1e}^{-1})_H \simeq 100$. This condition is approximately fulfilled for the other vanadium-based Laves phase hydrides in a wide range of x [13, 14]. The nearly constant ratio $(T_{1e}^{-1})_M/(T_{1e}^{-1})_H$ is typical for transition metal–hydrogen systems since both $(T_{1e}^{-1})_M$ and $(T_{1e}^{-1})_H$ are usually dominated by the d-band contribution [15]. In any case $(T_{1e}^{-1})_H$ is small compared with the measured proton relaxation rate in the vicinity of the peaks.

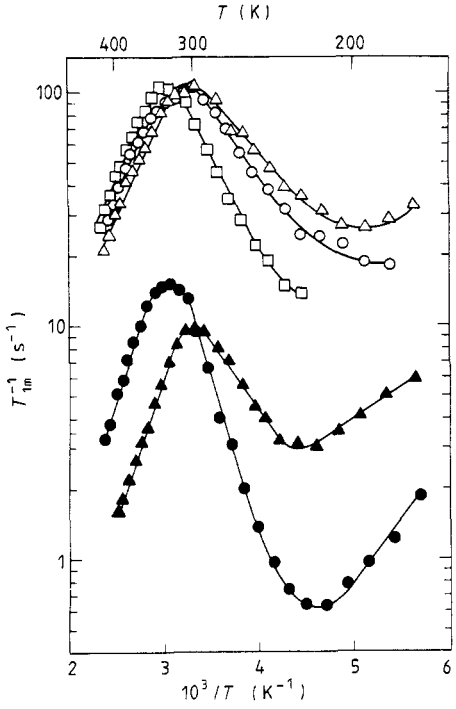

Figure 5. The dependence of the motional contributions to the ^1H and ^2D spin-lattice relaxation rates on reciprocal temperature for $TaV_2H_{0.22}$ (□), $TaV_2H_{0.87}$ (○), $TaV_2H_{1.33}$ (△), $TaV_2D_{0.50}$ (●) and $TaV_2D_{1.54}$ (▲). The relaxation rates are measured at 19.3 MHz (^1H) and 13.8 MHz (^2D).

Figure 5 shows the motional contributions $(T_{1m}^{-1})_H = (T_1^{-1})_H - (T_{1e}^{-1})_H$ for different samples as functions of reciprocal temperature in the high-T region. According to the BPP-type model of spin relaxation due to hydrogen diffusion, the $(T_{1m}^{-1})_H$ maximum is observed when $\omega\tau_d \simeq 1$, τ_d being a mean dwell time of H atom in an interstitial site; $(T_{1m}^{-1})_H$ is proportional to τ_d for $\omega\tau_d \ll 1$ (fast diffusion limit) and to $\omega^{-2}\tau_d^{-1}$ for $\omega\tau_d \gg 1$ (slow diffusion limit). If τ_d follows the Arrhenius relation,

$$\tau_d = \tau_{d0} \exp(E_a/k_B T) \tag{1}$$

a plot of $\log(T_{1m}^{-1})_H$ against T^{-1} is expected to be linear in the fast diffusion and slow diffusion limits with slopes E_a/k_B and $-E_a/k_B$, respectively, where E_a is the activation energy. As can be seen from figure 5, the experimental picture is more complicated. The

apparent activation energies obtained from the high-temperature and low-temperature slopes of $\log(T_{1m}^{-1})_H$ versus T^{-1} plots are not equal. The difference between the slopes is higher for the samples for which the low-T peak is closer to the high-T one. Therefore, the low-T peak may contribute to this difference. Tables 2 and 3 summarise the temperatures of the high-T and low-T maxima for ^{1}H relaxation rates and the maximum motional contributions $(T_{1m}^{-1})_H^{HTmax}$ and $(T_{1m}^{-1})_H^{LTmax}$ at different resonance frequencies. Most of the ^{1}H measurements in the high-T region have been made at 19.3 MHz since at low frequencies the motional contribution to the relaxation rate is higher. In the low-T region, where the free induction decay is short, the low-frequency measurements are somewhat restricted by the finite recovery time of the spectrometer after the RF pulse. Therefore, most of the low-T measurements have been made at higher frequencies, for which the recovery time is shorter. The ^{2}D spin-lattice relaxation rates in TaV_2D_x are also found to exhibit double-peak temperature dependences. The experimental $(T_1^{-1})_D$ data for the two TaV_2D_x samples in the high-T region are included in figure 5.

We now summarise the main features of our experimental results with respect to changes in H(D) concentration and resonance frequency and to hydrogen isotope substitution.

Table 2. Temperatures of the high-T proton relaxation rate maxima and the maximum motional relaxation rates, $(T_{1m}^{-1})_H^{HTmax}$, in TaV_2H_x.

Sample	Resonance frequency (MHz)	T_{HTmax} (K)	$(T_{1m}^{-1})_H^{HTmax}$ (s^{-1})
$TaV_2H_{0.22}$	19.3	328	105
$TaV_2H_{0.56}$	19.3	320	108
$TaV_2H_{0.70}$	19.3	320	100
$TaV_2H_{0.87}$	19.3	310	106
	90	356	21.5
$TaV_2H_{1.15}$	19.3	300	104
	90	346	23.7
$TaV_2H_{1.33}$	19.3	290	109

Table 3. Temperatures of the low-T proton relaxation rate maxima and the maximum motional relaxation rates, $(T_{1m}^{-1})_H^{LTmax}$, in TaV_2H_x.

Sample	Resonance frequency (MHz)	T_{LTmax} (K)	$(T_{1m}^{-1})_H^{LTmax}$ (s^{-1})
$TaV_2H_{0.56}$	64	90	4.0
$TaV_2H_{0.70}$	64	110	5.8
$TaV_2H_{0.87}$	31	92	14.5
	64	114	6.4
	90	125	4.9
$TaV_2H_{1.15}$	90	167	5.6
$TaV_2H_{1.33}$	64	167	9.1
	90	187	6.2

(i) As the hydrogen concentration increases, the position of the high-T relaxation rate maximum shifts to lower temperatures. This trend is clearly manifested in the ^{1}H, ^{2}D and ^{51}V data (figures 1, 3 and 5, tables 1 and 2). It implies that H(D) mobility increases with increase in x, at least at temperatures close to the high-T maxima. This kind of concentration dependence of mobility is quite unusual for metal–hydrogen systems.

(ii) For all the studied concentrations the high-T vanadium relaxation rate peak in the deuteride is shifted to higher temperatures from the one in the hydride with nearly the same x (figure 4, table 1). Since in both the hydride and the deuteride the dominant ^{51}V relaxation mechanism near the high-T peak is the same (electric quadrupole interaction modulated by H(D) diffusion) [16], the observed shift unambiguously indicates that the hopping rate of D atoms is lower than that of H atoms. Thus, the sign of the isotope effect in H(D) diffusion in TaV_2 is normal, at least at temperatures close to the high-T maxima.

(iii) The value of the high-T maximum relaxation rate $(T_{1m}^{-1})_H^{HTmax}$ is nearly constant in the whole studied range of x (figure 5, table 2). The insensitivity of $(T_{1m}^{-1})_H^{HTmax}$ to changes in the H content indicates that the H–H dipolar contribution to $(T_{1m}^{-1})_H$ is small, and the motional part of the proton relaxation rate is determined by H–V dipolar interactions. The concentration dependence of $(T_1^{-1})_V^{HTmax}$ has been discussed in [16].

(iv) The frequency dependence of $(T_{1m}^{-1})_H^{HTmax}$ is found to go as ω^{-1}, as expected in the BPP-type model of spin relaxation. Following the arguments of [5] and [17], we can conclude that the experimental data are not consistent with the existence of a continuous τ_d distribution of considerable width. As noted above, the localised motion of H atoms is likely to contribute to the observed difference between the high-T and low-T slopes of $\log(T_{1m}^{-1})_H$ versus T^{-1} plots (figure 5).

(v) As the H(D) concentration increases, the position of the low-T relaxation rate maximum shifts to higher temperatures (figures 1 and 3, tables 1 and 3). Thus, the characteristic frequency of the localised motion decreases with the increase in x.

(vi) The low-T vanadium relaxation rate peak in the deuteride is shifted to higher temperatures from the one in the hydride with nearly the same x (table 1). Thus, the characteristic frequency of the localised motion of D atoms is lower than that of H atoms. As noted above, the value of $(T_1^{-1})_V^{LTmax}$ for the deuterides is considerably higher than for the hydrides with nearly the same x. This means that the effective 'amplitude' of the localised motion of D atoms is higher than that of H atoms.

(vii) In contrast to $(T_{1m}^{-1})_H^{HTmax}$, the value of $(T_{1m}^{-1})_H^{LTmax}$ strongly increases with the increase in x (table 3). Since the motional part of the proton relaxation rate in TaV_2H_x is determined by H–V dipolar interaction, this trend indicates that the effective 'amplitude' of the localised motion grows with increasing H content.

(viii) The frequency dependence of $(T_{1m}^{-1})_H^{LTmax}$ goes approximately as ω^{-1}, and at the low-temperature slope of the low-T peak $(T_{1m}^{-1})_H$ is nearly proportional to ω^{-2} (figure 2, table 3). These results are inconsistent with the existence of a broad distribution of characteristic frequencies of the localised motion.

4. Discussion

4.1. Theoretical background

In order to make some quantitative conclusions from the measurements we consider the theoretical expressions for the proton spin-lattice relaxation rates. When long-range

diffusion coexists with localised motion with much higher hopping frequency, the motional part of the relaxation rate can be written as

$$(T_{1m}^{-1})_H = (T_{1d}^{-1})_H + (T_{1L}^{-1})_H \tag{2}$$

where $(T_{1d}^{-1})_H$ and $(T_{1L}^{-1})_H$ are the contributions due to hydrogen diffusion and localised motion, respectively. In TaV_2H_x the proton spin-lattice relaxation is mainly determined by H–V dipolar interaction. The estimates show that H–H dipolar contribution does not exceed 12% of the motional relaxation rate for the highest x. Neglecting the H–H contribution, $(T_{1d}^{-1})_H$ can be written as

$$(T_{1d}^{-1})_H = \frac{\gamma_H^2 M_2^{H-V}}{2\omega}(1-A)\left(\frac{\omega\tau_d}{1+(1-\alpha)^2\omega^2\tau_d^2} + \frac{3\omega\tau_d}{1+\omega^2\tau_d^2} + \frac{6\omega\tau_d}{1+(1+\alpha)^2\omega^2\tau_d^2}\right) \tag{3}$$

where $\alpha = \gamma_V/\gamma_H$, γ_V and γ_H are the gyromagnetic ratios for ^{51}V and ^1H, respectively, M_2^{H-V} is the H–V dipolar contribution to the rigid-lattice second moment of the ^1H NMR line, and A is the fraction of M_2^{H-V} that is averaged out by localised motion. We assume that the correlation functions for fluctuating dipolar fields are decaying exponentially.

For hydrogen atom hopping between the two wells of equal depth $(T_{1L}^{-1})_H$ is given by [8]

$$(T_{1L}^{-1})_H = \frac{\gamma_H^2 M_2^{H-V}}{2\omega} A\left(\frac{\omega\tau_L}{1+(1-\alpha)^2\omega^2\tau_L^2} + \frac{3\omega\tau_L}{1+\omega^2\tau_L^2} + \frac{6\omega\tau_L}{1+(1+\alpha)^2\omega^2\tau_L^2}\right) \tag{4}$$

where τ_L is the average period of hopping. Comparing equations (3) and (4) it is easy to see that the ratio of the maximum relaxation rates for the low-T and high-T peaks is determined by the value of $A/(1-A)$. For a hydrogen atom hopping between sites 1 and 2 it can be shown using the analysis of [18] that

$$1 - A = \tfrac{1}{4}\sum_i X_i r_{1i}^{-6} \Big/ \sum_i r_{1i}^{-6}$$
$$X_i = (r_{1i}/r_{2i})^6 + (r_{1i}/r_{2i})^3 (3\cos^2\beta_i - 1) + 1 \tag{5}$$

where β_i is the angle between the vectors $\boldsymbol{r}_{1i}$ and $\boldsymbol{r}_{2i}$ connecting the ith V nucleus with sites 1 and 2. Equation (5) is written in the powder averaged form. Thus, for a given τ_L and the crystallographic model of localised motion it is possible to calculate $(T_{1L}^{-1})_H$ using equations (4) and (5).

The theoretical analysis of spin–lattice relaxation for ^2D and ^{51}V is a more complex problem, since for these nuclei the motional relaxation rate is usually dominated by quadrupole interaction. Assuming that a spin temperature is maintained in the system, the quadrupole contribution to the relaxation rate may be written in the general form

$$T_{1Q}^{-1} = f\langle\Delta\nu_Q^2\rangle J(\omega, \tau_c) \tag{6}$$

where $\langle\Delta\nu_Q^2\rangle$ is the mean square value of the fluctuating part of the quadrupole interaction parameter, $J(\omega, \tau_c)$ is the spectral density function for EFG fluctuations and f is a factor depending on nuclear spin. In contrast to the case of dipole–dipole interaction, the correlation time τ_c for quadrupole interaction may not coincide [19] with $\tau_d/2$ or τ_d. Therefore, a reliable estimate of τ_{d0} can hardly be obtained from ^2D relaxation data, although the value of E_a for deuterium diffusion can still be found from these measurements. The theoretical estimation of $\langle\Delta\nu_Q^2\rangle$ is also problematic since it requires knowledge of the spatial charge distribution and the Sternheimer anti-shielding factor. In the

following we shall employ the experimental data on ^{2}D and ^{51}V relaxation only for the qualitative analysis of H(D) motion in TaV_2.

4.2. Application to the measurements

In principle, the proton relaxation rate data can be analysed in terms of equations (3) and (4) to obtain the temperature dependences of τ_d and τ_L. However, in the temperature range between the two relaxation rate peaks both the long-range diffusion and the localised motion are expected to give non-negligible contributions to the measured $(T_1^{-1})_H$. Therefore, some additional assumptions are required to separate $(T_{1d}^{-1})_H$ and $(T_{1L}^{-1})_H$. The temperature dependence of τ_d usually follows the Arrhenius relation, equation (1). Since the frequency dependence of $(T_{1m}^{-1})_H^{HTmax}$ is not consistent with the existence of a broad τ_d distribution, we assume that at each T there is a single τ_d value determined by equation (1). The observed difference between the high-temperature and low-temperature slopes of $\log(T_{1m}^{-1})_H$ versus T^{-1} plots (figure 5) can be attributed to the effects of localised motion. This assumption allows one to separate $(T_{1d}^{-1})_H$ and $(T_{1L}^{-1})_H$ in the region between the peaks. By fitting equations (3) and (1) to the high-temperature portion of the measured $(T_{1m}^{-1})_H$ we can obtain the values of E_a and τ_{d0}. Using these values $(T_{1d}^{-1})_H$ is calculated in the whole temperature range, and $(T_{1L}^{-1})_H$ is estimated by subtracting $(T_{1d}^{-1})_H$ from $(T_{1m}^{-1})_H$.

The values of E_a and τ_{d0} obtained from the high-temperature proton relaxation data at 19.3 MHz are listed in table 4. It can be seen that E_a tends to decrease with increasing hydrogen content. This is compatible with the observed increase of the hydrogen hopping rate at $T \simeq 300$ K with increasing x. Table 4 also includes the E_a values for deuterium diffusion in $TaV_2D_{0.50}$ and $TaV_2D_{1.54}$ obtained from the high-temperature ^{2}D relaxation data. Comparison of the E_a values for the hydrides and the deuterides with similar x shows that $E_a^D > E_a^H$. The sign of the isotope effect in E_a for the TaV_2–H(D) system is opposite to the one observed for HfV_2–H(D) and ZrV_2–H(D) with high H(D) concentrations [4].

Table 4. Hydrogen and deuterium diffusion parameters resulting from the fit of equations (3) and (1) to the high-temperature relaxation rate data at 19.3 MHz (^{1}H) and 13.8 MHz (^{2}D).

Sample	E_a (eV)	τ_{d0} (10^{-12} s)
$TaV_2H_{0.22}$	0.23	2.5
$TaV_2H_{0.56}$	0.24	1.1
$TaV_2H_{0.70}$	0.23	1.6
$TaV_2H_{0.87}$	0.21	2.7
$TaV_2H_{1.15}$	0.22	1.8
$TaV_2H_{1.33}$	0.21	1.7
$TaV_2D_{0.50}$	0.26	
$TaV_2D_{1.54}$	0.23	

As remarked in section 3, the frequency dependence of the proton relaxation rate at low temperatures is not consistent with the existence of a broad distribution of τ_L values. This is in contrast to the data for α-ScH_x [8] showing much weaker frequency

dependences of $(T_{1m}^{-1})_H$ at low temperatures. Note that if the localised motion is due to some kind of tunnelling the temperature dependence of τ_L may have nothing in common with the Arrhenius-type behaviour. We obtain $\tau_L(T)$ by fitting the $(T_{1L}^{-1})_H$ data to equation (4) with AM_2^{H-V} fixed to give the experimental value of $(T_{1L}^{-1})_H^{LTmax}$. The resulting temperature dependences of τ_L for the three TaV_2H_x samples are shown in figure 6. It should be noted that the $\tau_L(T)$ data obtained from the measurements at different frequencies are nearly the same. For all the studied samples $\tau_L(T)$ can be fitted by the exponential functions

$$\tau_L = \tau_{L0} \exp(-T/T_0) \tag{7}$$

shown as full lines in figure 6. The resulting fitting parameters T_0 and τ_{L0} are listed in table 5. T_0 appears to be nearly the same for different x, and τ_{L0} strongly increases with increasing H content. As shown in figure 6, $\tau_L(T)$ can be described by equation (7) up

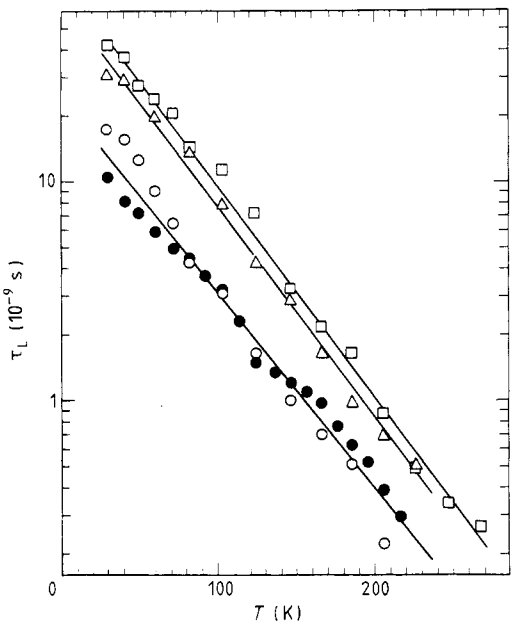

Figure 6. The temperature dependence of τ_L for $TaV_2H_{0.87}$ (○, ●), $TaV_2H_{1.15}$ (△) and $TaV_2H_{1.33}$ (□). The τ_L values are obtained from the measurements at 64 MHz (●) and 90 MHz (○, △, □).

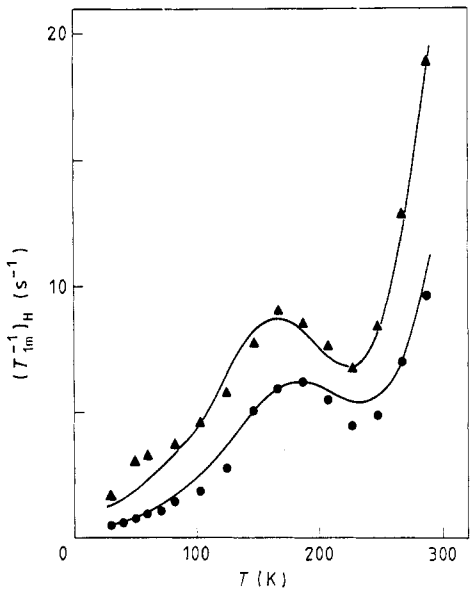

Figure 7. The temperature dependence of the ^1H spin-lattice relaxation rate in $TaV_2H_{1.33}$ at 64 (▲) and 90 MHz (●). The full curves show the fit to the data based on equations (3) and (4).

to temperatures considerably exceeding those of the low-T maxima. This may serve as evidence in favour of the model used to separate $(T_{1L}^{-1})_H$ and $(T_{1d}^{-1})_H$ in the region between the two peaks. As a further example, figure 7 shows the $(T_{1m}^{-1})_H$ data and the fit for $TaV_2H_{1.33}$ at 64 and 90 MHz. The fit is based on equations (3) and (4) with $\tau_d(T)$ and $\tau_L(T)$ determined by equations (1) and (7), respectively. A single set of fitting parameters is used for both resonance frequencies, the values of τ_{d0}, E_a, τ_{L0} and T_0 being specified in tables 4 and 5.

Table 5. Parameters of the low-temperature localised motion of H atoms resulting from the fit of equations (4) and (7) to the proton relaxation rate data.

Sample	T_0 (K)	τ_{L0} (10^{-8} s)
$TaV_2H_{0.56}$	50.3	0.89
$TaV_2H_{0.87}$	49.8[a]	2.7[a]
$TaV_2H_{1.15}$	45.0	7.1
$TaV_2H_{1.33}$	44.8	9.2

[a] Obtained from the data at three resonance frequencies.

The temperature dependence of τ_L given by equation (7) is quite unusual. At low temperatures this dependence is much weaker than the Arrhenius one. It is interesting to note that a similar exponential temperature dependence has also been observed for electrical resistivity of some metallic glasses [20] at low temperatures. The behaviour of hydrogen in a two-well potential is likely to have the features of the two-level system model [21], which is used to describe the physical properties of glasses. Hence, one may expect the typical 'glassy' features in the electrical resistivity and heat capacity of $TaV_2H_x(D_x)$ at low temperatures. For the related system $ZrV_2H_{3.85}$ Vajda *et al* [22] have recently reported on the existence of a resistivity minimum near 17 K.

We now consider the possible crystallographic models of the localised motion. Figure 8 shows the (1 1 0) plane of $TaV_2H_x(D_x)$ with interstitial g- and e-sites. The out-of-plane V atoms and g-sites which are the nearest neighbours of the site G_1 are also included in figure 8. Using equation (5) we can calculate the values of $A/(1-A)$ for different models of hopping and compare them with the experimental values of $(T_{1m}^{-1})_H^{LTmax}/(T_{1m}^{-1})_H^{HTmax}$. For hopping between the nearest g-sites ($G_1 \leftrightarrow G_2$ or $G_1 \leftrightarrow G_3(G_4)$) and between g- and e-sites ($G_1 \leftrightarrow E_1$) the calculated values of $A/(1-A)$ are 0.61, 0.41 and 0.37, respectively. The experimental values of $(T_{1m}^{-1})_H^{LTmax}/(T_{1m}^{-1})_H^{HTmax}$ change from 0.12 for $x = 0.56$ ^ 26 for $x = 1.33$. Leaving aside the numerical difference between the calculated and experimental values, the model cannot explain the concentration dependence of $(T_{1m}^{-1})_H^{LTmax}$. Furthermore, the model of hopping between the nearest interstitial sites cannot account for the observed strong

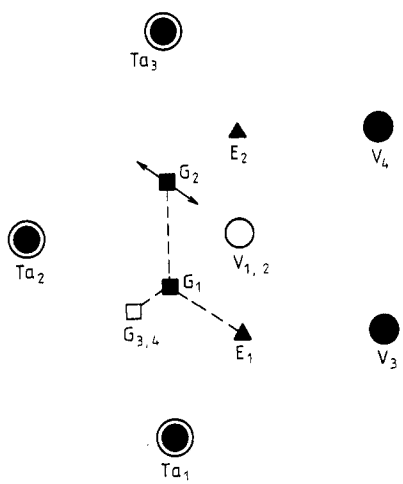

Figure 8. The (1 1 0) plane of TaV_2 with g-sites (G_1, G_2) and e-sites (E_1, E_2). The in-plane sites are shown by full symbols. The projections of the out-of-plane V atoms (V_1, V_2) and g-sites (G_3, G_4) are shown by open symbols. The broken lines indicate the possible ways of hopping between the nearest interstitial sites. The arrows show the directions of H(D) atom displacements, which are most effective for modulation of H–V dipolar interactions.

isotope effect in $(T_{1m}^{-1})_V^{LTmax}$, since for such hopping of H(D) atoms the amplitude of EFG fluctuations on V nuclei is expected to be the same for both isotopes.

Before turning to the discussion of the alternative crystallographic model of the localised motion we consider two possible mechanisms which might be responsible for the observed concentration dependence of $(T_{1m}^{-1})_H^{LTmax}$. (i) Only a fraction of H atoms may participate in the localised motion. In this case a single value of the relaxation rate may result from the fast spin diffusion, and the growth of $(T_{1m}^{-1})_H^{LTmax}$ with increasing x may be explained by the increase in the fraction of mobile H atoms. If this is the case, $(T_{1m}^{-1})_V^{LTmax}$ as a function of x is expected to grow considerably faster than $(T_{1m}^{-1})_H^{LTmax}$ (at least, at low x), since for the host-metal relaxation the changes both in the fraction of mobile atoms and in the total concentration x itself would contribute to the mean amplitude of EFG fluctuations. However, as can be seen from tables 1 and 3, the relative changes in $(T_{1m}^{-1})_H^{LTmax}$ and $(T_{1m}^{-1})_V^{LTmax}$ with H(D) concentration are nearly the same. (ii) Hydrogen atoms may jump between two wells of different depths. In this case the right-hand side of equation (4) should be multiplied [8] by $\mathrm{sech}^2(\Delta/2k_BT)$, where Δ is the energy difference between the bottom of the wells. Hence, for hopping between the nearest interstitial sites the growth of $(T_{1m}^{-1})_H^{LTmax}$ with increasing x might be ascribed to the decrease in Δ. However, the opposite concentration dependence of Δ is expected, since the energy asymmetry of the two wells is believed to result from interactions with other H atoms [23]. Thus, these two mechanisms modifying the model of hopping between the nearest interstitial sites cannot provide a consistent description of the experimental data.

The alternative model of the localised motion implies the hopping of an H(D) atom between two (or more) displaced sites within a tetrahedral interstitial. In this case the concentration dependence of $(T_{1m}^{-1})_H^{LTmax}$ can be naturally explained by the increase in the 'amplitude' of intra-site motion with increasing H content. Since the EFG values at V sites are very sensitive to V–H(D) distances, the strong difference between the $(T_{1m}^{-1})_V^{LTmax}$ for hydrides and deuterides can be attributed to the difference in displacements of hydrogen isotopes, the displacement amplitude of D atoms being higher than that of H atoms. We have estimated $A/(1-A)$ for different directions of intra-site displacements. Displacements from a g-site in the directions of the nearest g- and e-sites are found to give too small $A/(1-A)$ values to account for the experimental data. The most effective displacements for modulation of H–V dipolar interactions are those along the line connecting the centres of Ta–Ta and V–V edges. These displacements are shown in figure 8 by arrows. In order to account for the experimental value of $(T_{1m}^{-1})_H^{LTmax}/(T_{1m}^{-1})_H^{HTmax}$ for $x = 1.33$ the amplitude of these displacements should be ± 0.11 Å if they are assumed to be symmetrical with respect to G_2. This value of the amplitude seems to be reasonable. Note that according to the neutron diffraction data [11] at room temperature D atoms in $TaV_2D_{1.6}$ are displaced by 0.1 Å from geometrical centres of g-sites to the centres of Ta–Ta edges. Thus, the model of H(D) hopping between displaced sites within the same interstitial can, in principle, account for all the experimental features. However, the location of the displaced sites can hardly be determined from NMR data. The spatial aspects of the localised motion may be clarified by neutron scattering experiments.

5. Concluding remarks

The additional low-temperature maximum of the spin-lattice relaxation rate in

$TaV_2H_x(D_x)$ unambiguously indicates the existence of fast localised motion of H(D) atoms, which is not frozen on the NMR frequency scale down to 10 K. The temperature dependence of the frequency of the localised motion is non-Arrhenius, and in the range 30–280 K it can be described by the exponential law, $\tau_L^{-1} \sim \exp(T/T_0)$. As the H(D) concentration increases, the effective amplitude of the localised motion increases and its frequency decreases. The observed strong isotope effects at low temperatures suggest a quantum origin of the localised motion. Similar phenomena may also be found in the other Laves phase hydrides. If the characteristic frequencies of the localised motion are lower than in the case of $TaV_2H_x(D_x)$ the additional T_1^{-1} maximum may not appear merging into the low-temperature slope of the diffusion-induced relaxation rate peak. This is probably the case for $HfV_2H_x(D_x)$, $ZrV_2H_x(D_x)$ and $ZrTi_2H_x(D_x)$, where the additional T_1^{-1} maximum is absent, but still there is an anomalous frequency dependence of T_1^{-1} at $T < 130$ K [5, 24].

The unusual concentration dependence of the hydrogen diffusion rate in $TaV_2H_x(D_x)$ may also be related with the presence of localised motion. The effects of intra-site dynamics of hydrogen on its inter-site motion have been recently considered by Teichler [25] in the framework of phonon-assisted hydrogen tunnelling. Although his analysis is not strictly applicable to our case, it shows that such effects may be important in metal–hydrogen systems.

Acknowledgments

We are grateful to M E Kost and L N Padurets for help with sample preparation, and to V A Somenkov and A V Irodova for useful discussions.

References

[1] Bowman R C, Craft B D, Attalla A and Johnson J R 1983 *Int. J. Hydrogen Energy* **8** 801
[2] Shinar J, Davidov D and Shaltiel D 1984 *Phys. Rev.* B **30** 6331
[3] Belyaev M Yu, Skripov A V, Kozhanov V N and Stepanov A P 1984 *Sov. Phys.–Solid State* **26** 1285
[4] Skripov A V, Belyaev M Yu, Rychkova S V and Stepanov A P 1987 *Fiz. Tverd. Tela* **29** 3160
[5] Skripov A V, Rychkova S V, Belyaev M Yu and Stepanov A P 1989 *Solid State Commun.* **71** 1119
[6] Skripov A V, Belyaev M Yu, Rychkova S V, Stepanov A P and Romanov E P 1988 *Fiz. Tverd. Tela* **30** 587
[7] Skripov A V, Belyaev M Yu, Rychkova S V and Stepanov A P 1989 *J. Phys.: Condens. Matter* **1** 2121
[8] Lichty L R, Han J W, Ibanez-Meier R, Torgeson D R, Barnes R G, Seymour E F W and Sholl C A 1989 *Phys. Rev.* B **39** 2012
[9] Torgeson D R, Han J W, Chang P C T, Lichty L R, Barnes R G, Seymour E F W and West G W 1989 *Z. Phys. Chem.* **164** 853
[10] Lynch J F 1981 *J. Phys. Chem. Solids* **42** 411
[11] Somenkov V A and Irodova A V 1984 *J. Less-Common Met.* **101** 481 and private communication
[12] Bloembergen N, Purcell E M and Pound R V 1948 *Phys. Rev.* **73** 679
[13] Belyaev M Yu, Skripov A V, Stepanov A P and Galoshina E V 1987 *Fiz. Metal. Metalloved.* **63** 905
[14] Stepanov A P, Skripov A V and Belyaev M Yu 1989 *Z. Phys. Chem.* **163** 603
[15] Cotts R M 1978 *Hydrogen in Metals I* ed G Alefeld and J Völkl (Berlin: Springer) ch 9
[16] Skripov A V, Belyaev M Yu and Stepanov A P 1989 *Solid State Commun.* **71** 321
[17] Markert J T, Cotts E J and Cotts R M 1988 *Phys. Rev.* B **37** 6446
[18] Gabuda S P and Lundin A G 1986 *Internal Mobility in Solid State* (Novosibirsk: Nauka) p 43
[19] Seymour E F W 1982 *J. Less-Common Met.* **88** 323
[20] Varyukhin S V and Egorov V S 1987 *Fiz. Metal. Metalloved.* **63** 1127

[21] Phillips W A 1987 *Rep. Prog. Phys.* **50** 1657
[22] Vajda P, Daou J N, Burger J P, Shaltiel D and Grayevsky A 1989 *Z. Phys. Chem.* **163** 75
[23] Cannelli G, Cantelli R and Cordero F 1989 *Z. Phys. Chem.* **164** 943
[24] Skripov A V, Rychkova S V, Belyaev M Yu and Stepanov A P 1990 submitted to *J. Phys.: Condens. Matter*
[25] Teichler H 1989 *Z. Phys. Chem.* **164** 747